Hindawi
Mathematical Problems in Engineering
Volume 2019, Article ID 3596784, 11 pages
https://doi.org/10.1155/2019/3596784

Research Article

An Event-Triggered Robust Control and Bandwidth Scheduling Codesign Approach for Networked Control Systems with Uncertain Time Delays

Yun Niu and Yalin Liang

School of Marine Science and Technology, Northwestern Polytechnical University, Shaanxi 710072, China

Correspondence should be addressed to Yun Niu; niuyun010121@nwpu.edu.cn

Received 10 October 2018; Revised 6 January 2019; Accepted 30 January 2019; Published 27 February 2019

Academic Editor: Leonardo Acho

For networked control systems, the bandwidth resource is always limited; thus besides control performance, the efficient resource utilization is also crucial. In this paper, a novel event-triggered control and resource scheduling codesign approach is proposed to stabilize the uncertain dynamic systems which are subject to time-varying network introduced delays. A discrete switched system with uncertain parameters is employed to model the event-triggered control system with time-varying network-induced delays. Based on the model, a control law, scheduling strategy, and event-triggered condition codesign approach is investigated. A set of linear matrix inequalities are used to tackle the codesign problem. As the solution to the problem, a control law is obtained to guarantee stability or certain performance properties; an event-triggered condition and a scheduling strategy are also obtained to efficiently utilize the limited resources. That is, the event-triggered condition makes the network accession be triggered when it is necessary. The scheduling strategy guarantees the control loop suffering the worst control performance can get the authority to access the network. The proposed approach is evaluated through simulated experiments, with respect to the networked control of inverted pendulums. The results show that the proposed event-triggered control and scheduling approach can achieve better control performances with lower average resource consumption in comparison with the time-based control strategy.

1. Introduction

Networked control systems (NCS) generally consist of controllers, corresponding sensor, and actuator nodes which are always connected via a field-bus or industrial wireless network [1]. This type of structure brings many attractive advantages including reduced wiring, easy maintenance, and restructuring, but the challenges caused by unideal communication through the network can not be ignored. Especially, the limitation of the communication bandwidth and computation capacity is quite challenging. The resource limitation mentioned above can cause time-varying communication delays, unequal sampling intervals, and packet dropouts which always lead to a decline in control performances. In order to surmount these problems, the control system design should take into account not only control performances but also the resource scheduling.

Control and scheduling codesign methods have been widely studied recently and those used in previous literature can roughly be classified into two types, i.e., the time-based codesign method and the event-based one. The difference between these two methods lie in the fact that the data transmission and control updating are triggered periodically using the time-based codesign method but by events when the event-based method is used.

The time-based codesign approaches can be further classified by static and dynamic application from the scheduling perspective. Based on the static scheduling strategy, the schedule was calculated offline, where the periodic schedules were usually employed. In [2, 3], the design of scheduling and control strategy was formulated as an integrated quadratic programming problem and the solution was calculated before the runtime. In [4], a new state which describes the scheduling performance was augmented to the original state-space, and an exponential function of control error was

utilized to dynamically allocate the bandwidth. In [5], an optimal bandwidth allocation strategy for distributed axes control was introduced to enhance the robot tracking within the bandwidth range. Based on the dynamic scheduling strategy, the schedule was calculated online according to the measurements of certain control performances. In [6], an online nonpreemptive scheduling policy was employed. The scheduling policy minimized a quadratic performance criterion for the overall system. In [7], a robust receding-horizon control and scheduling problem with a quadratic performance criterion was introduced and solved based on the dynamic programming. In [8], periods of controller tasks integrated into a uniprocessor system were optimized online related to both the control performance and real-time schedulability analysis. The Lagrange multipliers and gradient descent method were used to optimize the periods of controller tasks online, and the method could yield near-optimal results with a short running time.

Although the aforementioned time-based codesign approaches are preferred from the perspective of analysis and design, the overall resource consumption of the system may be still quite challenging because of the coming characters. The time-based codesign approaches require feeding measurements from all plants at each sampling instant no matter whether the system is operating desirably or not. This is clearly a waste of communication resources. This is especially disadvantageous in applications where the measured data or the control commands have to be transmitted over a shared communication network whose bandwidth or power is constrained.

To improve the resource consumption, the event-based control framework has been developed as a way to solve the problem of resource constraints. In the event-based control framework, the data transmission instants are no longer respected to a prefixed interval but rather to the stability or performance purposes. Namely, the data transmission of a system is not triggered periodically but only when some events occur according to the designed event-trigger strategy.

One crucial problem solved by the event-based control methods is how to analyze and design NCS with event-triggering conditions. Heemels [9] firstly employed an introductory event-driven PID controller example to illustrate the achievable reduction of control computations (up to 80%) and then provided an event-driven control scheme for perturbed linear systems. They also presented computational means and tuning rules that support the design of the event-triggered control laws in case of nonuniform sampling and uniform sampling. The control performances were expressed in terms of ultimate bounds and convergence rates to these bounds. Based on the event-driven control scheme proposed above, Heemels and Donkers [10] present two frameworks based on perturbed linear and piecewise linear systems, leading to conditions for global exponential stability and ℓ_2-gain performance of the resulting closed-loop systems in terms of linear matrix inequalities. Observer-based controllers for linear systems and advanced event-triggering mechanisms (ETMs) that could reduce communication in both the sensor-to-controller channels and the controller-to-actuator channels were also proposed.

Beside the linear systems, the event-triggered control framework can also be used in nonlinear systems. Girard presented a new class of dynamic triggering mechanisms that use an additional internal dynamic variable, the stability of the resulting event-triggered closed-loop system was proved, and the influence of design parameters on the decay rate of the Lyapunov function was also discussed [11]. Romain Postoyan et al. proposed a framework for the event-triggered stabilization of nonlinear systems using hybrid systems tools [12]. By reformulating the nonlinear NCSs as an event-triggered networked T-S fuzzy systems with time-varying delays, Songlin Hu et al. proposed a codesign algorithm for determining the gain of the fuzzy controller and the triggering parameters simultaneously [13]. Zhang et al. considered the problems of multitarget selection and formation for multiagent systems in [14]; an event-triggered mode was applied to reduce the communication links between agents.

Besides the analysis and synthesis for NCS with event-triggering conditions, another nontrivial problem should be solved by the event-based control methods is how to exclude the Zeno behavior (the occurrence of an infinite number of events in finite time) in the presence of disturbances. The approaches used to handle this problem roughly fall into two categories. The one is to design an event-triggering mechanism (ETM) in such a way that global asymptotic stability and/or certain type of control performances are guaranteed with a positive minimum interevent time (MIET) in absence of disturbances [15], the other is the so-called periodic event-triggered control (PETC) proposed by Heemels [16]. In PETC, the event-triggering condition is verified periodically and at every sampling time it is decided whether or not to transmit new measurements and to calculate new control signals. It is obvious that the PETC could guarantee the minimum interevent time of (at least) the sampling interval of the event-triggering condition. Furthermore, the periodic character of the triggering conditions also leads to the implementation benefits in discrete NCSs.

Those methods mentioned above mainly focused on designing the control laws in the presence of different event-triggering conditions. The proposed strategies could guarantee the stability of NCS with good control performances; however, the feasibility consideration in the bandwidth scheduling aspect was missing. Therefore, the event-based joint design strategy of resource scheduling and control has been proposed and still under research. In [17, 18] only the basic concepts of the issue was given. In [17], by considering a set of time-triggered or event-triggered control loops closed over a shared communication network, the minimum-variance control performances under various MAC protocols, including TDMA, FDMA, and CSMA, were studied and compared, and the results of the comparison showed that the event-based control and scheduling obtain better overall performance under the constrained bandwidth resource and the event-triggered control under CSMA gave the best performance throughout, whereas, in [19], the experiment results showed that, for the collision recovery access protocols (there is no scheduling strategy; packets are only lost due to collisions) such as pure ALOHA, if packets are transmitted whenever the event-based control generates

an event, the packet losses due to collisions might drastically reduce the performance of event-based control, and the time slot method employed by the time-triggered control policy could partly restrain the collisions; thus, in this situation time-triggered control was superior to event-based control. This result in fact emphasized the necessity of the codesign of control and scheduling for an improved control performance in the event-based framework. The approach [20] modeled the networked control system as a discrete-time switched system under the effect of Try-once-Discard (TOD) dynamic scheduling strategy, and a state feedback controller design method was given to guarantee the asymptotic stability of the closed-loop system by using LMI approach. However, the work does not consider the constraints induced by the event generator. Reference [21] proposed a method involved a joint design of an event-based control and scheduling strategy for improving the control performance and using the limited resources efficiently, but the work neglected the uncertain issues from resource competition. Meanwhile, lots of existing event-trigger based control and scheduling codesign methods needed a centralized scheduler to arbitrate the authority of network accession, e.g., [20–22], which might induce higher scheduling overhead.

In this paper, a novel systematic codesign method of control law, resource scheduling, and periodic event-triggering mechanism is proposed. The discrete-time switched system with parameter uncertainties is employed to model the event-based networked control system with uncertain delays. Furthermore, by using the Lyapunov function with a quadratic structure, the codesign problem can be solved in a linear matrix inequality (LMI) framework. A state feedback control law and the corresponding event-trigger condition is achieved from the solution. The scheduling strategy of the packet transmission is also proposed according to the event-trigger condition. The main contributions of our work are summarized as follows:

(i) An analysis model is proposed which describes both resource constraints induced challenges and event-trigger induced challenges.

(ii) A novel event-triggered control and scheduling codesign based on the LMIs approach is studied, which takes both network-induced uncertain communication delay and the event-triggering condition into account.

(iii) A low overhead distributed scheduling strategy is also given. The arbitration mechanisms of the scheduling strategy can be directly used by priority-driven networks such as controller area network (CAN).

Remark 1. In view of existing results, the network blocking induced transmission time out is the main cause of the packet drops in NCS [23]. Our research is focused on the codesign approach of control gain, bandwidth scheduling, and event-triggering condition. The network scheduler and the event-triggering condition we designed could guarantee that, at any time, the plant with worst control performance, namely, with the largest weighted Euclidean norm of the states has the authority to access the network and close its feedback control loop while the remainder plants run without updating their control inputs. The network scheduler can also guarantee that the network-induced delays are not larger than the "event-triggered" sampling time by restricting the bandwidth utilization. It is means that the packet drops induced by the transmission time out rarely happen. Therefore, we can obtain less conservative results via the proposed event-triggered control and bandwidth scheduling codesign approach, because the packet drops compensation methods, whether asynchronous dynamic based or Markovian jump methods, always cause more conservative results.

The rest of this paper is organized as follows: Section 2 formulates the system model for analysis. Section 3 gives the details of proposed event-based control and scheduling codesign procedure, and also the detailed overall stability proof. Finally, Section 4 presents simulation experiments to verify performance of our method.

2. System Model

2.1. System Architecture. Consider the NCS shown in Figure 1. The system consists of a set of plants $\mathbb{P} = \{P_i, i = 1, \ldots, N\}$ which are controlled by a shared processor via network communication. In each control loop, the sensors measure the states of the plant periodically as h_i, but whether transmitting the new measurements through the network at instant k is triggered by the event generators $\sigma_i(k), i = 1, \ldots, n$. The scheduler $\delta(k)$ is employed to arbitrate which control loop can access the network at the instant k. $\delta(k)$ can be 0 which means no transmission of the new measurements and corresponding control updates are performed at the current instant. Meanwhile, τ_{sc} and τ_{ca} represent the sensor-to-controller and the controller-to-actuator time-varying delay, respectively, due to the resource competition.

2.2. System Discretization. The controlled plant in our research can be described by a linear time-invariant system with uncertain transmission delay $\tau(t)$:

$$\dot{x}(t) = A_c x(t) + B_c u(t - \tau(t)) \tag{1}$$

where $x \in \mathbb{R}^n$ and $u(t - \tau(t)) \in \mathbb{R}^m$ are the state vector and the control input vector, respectively. $A_c \in \mathbb{R}^{n*n}$, $B_c \in \mathbb{R}^{n*m}$ are constant matrices with appropriate dimensions. Note that $\tau(t) = \tau_{sa}(t) + \tau_{ca}(t)$ is time-varying, and we assume that $0 \leq \tau(t) \leq h$, which can be guaranteed by an appropriated bandwidth scheduling strategy. h means the state measurement period.

Considering the event-trigger mechanism, if the control loop i obtains the authority to access the network, the control input vector will be updated within the sampling interval $t_k \leq t < t_{k+1}$, i.e.,

$$u(t - \tau(t)) = \begin{cases} u(t_{k-1}) & t_k \leq t < t_k + \tau_k \\ u(t_k) & t_k + \tau_k \leq t < t_{k+1} \end{cases} \tag{2}$$

where we set $t_{k+1} = t_k + h_i(k)$, in which $h_i(k)$ means the sample period of the control loop i at current instant k.

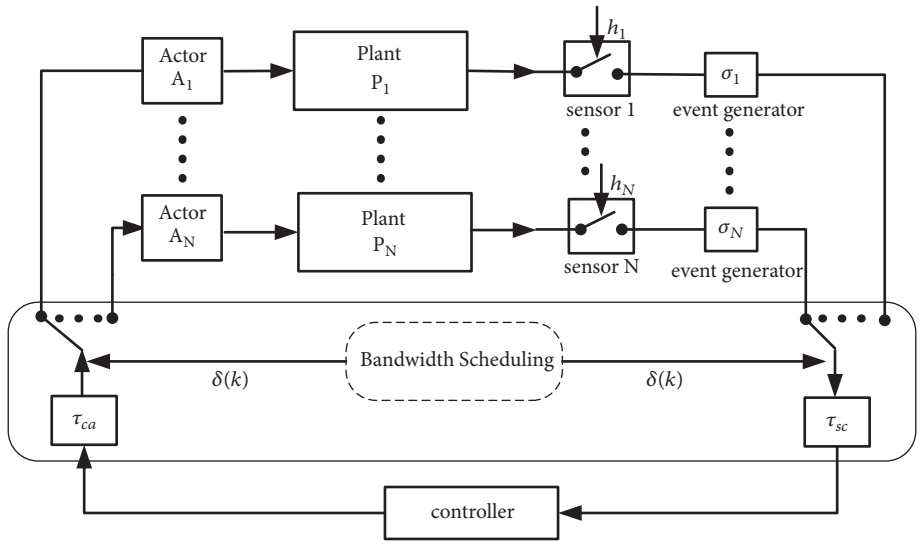

Figure 1: The diagram of the event-triggered networked control system.

If the packets transmission of the control loop has not been triggered, the control input vector will remain its previous status during the sampling interval, i.e.,

$$u(t-\tau(t)) = u(t_{k-1}) \quad t_k \le t < t_{k+1} \tag{3}$$

Considering the transmission behavior in (2), the discrete model of system in (1) can be formulated as [24]

$$\begin{aligned}\mathbf{x}(k+1) &= \mathbf{\Phi}(h)\mathbf{x}(k) + \mathbf{\Gamma}_0(h,\tau_k)\mathbf{u}(k) \\ &\quad + \mathbf{\Gamma}_1(h,\tau_k)\mathbf{u}(k-1)\end{aligned} \tag{4}$$

where $\mathbf{\Phi}(h) = e^{\mathbf{A}_c h}$, $\mathbf{\Gamma}_0(h,\tau_k) = \int_0^{h-\tau_k} e^{\mathbf{A}_c s} ds \mathbf{B}_c$, $\mathbf{\Gamma}_1(h,\tau_k) = \int_{h-\tau_k}^{h} e^{\mathbf{A}_c s} ds \mathbf{B}_c$

Let $\mathbf{z}(k) = \left(\mathbf{x}^T(k) \;\; \mathbf{u}^T(k-1)\right)^T$; we have

$$\begin{aligned}\mathbf{z}(k+1) &= \mathbf{A}_{d1}\mathbf{z}(k) + \mathbf{B}_{d1}\mathbf{u}(k) \\ &= \begin{bmatrix}\mathbf{\Phi}(h) & \mathbf{\Gamma}_1(h,\tau_k) \\ \mathbf{0} & \mathbf{0}\end{bmatrix}\mathbf{z}(k) \\ &\quad + \begin{bmatrix}\mathbf{\Gamma}_0(h,\tau_k) \\ \mathbf{I}\end{bmatrix}\mathbf{u}(k)\end{aligned} \tag{5}$$

where I denotes the identity matrix with appropriate dimensions.

Furthermore, considering the updating of the control input vector in (3), the discrete model of system in (1) can be formulated as

$$\begin{aligned}\mathbf{z}(k+1) &= \mathbf{A}_{d2}\mathbf{z}(k) + \mathbf{B}_{d2}\mathbf{u}(k) \\ &= \begin{bmatrix}\mathbf{\Phi}(h) & \mathbf{\Gamma}_1(h) \\ \mathbf{0} & \mathbf{0}\end{bmatrix}\mathbf{z}(k) + \begin{bmatrix}\mathbf{0} \\ \mathbf{I}\end{bmatrix}\mathbf{u}(k)\end{aligned} \tag{6}$$

where $\mathbf{\Gamma}_1(h) = \int_0^h e^{\mathbf{A}_c s} ds \mathbf{B}_c$.

Since the $\tau_k \in [0,h]$ is a uncertain variable, both $\mathbf{A}_{d1}$ and $\mathbf{B}_{d1}$ are uncertain matrices. Let $\widehat{\tau}_k \in [-h/2, h/2]$, $\widehat{\mathbf{\Gamma}}_0 = \int_0^{h/2} e^{\mathbf{A}_c s} ds \mathbf{B}_c$, $\widehat{\mathbf{\Gamma}}_1 = \int_{h/2}^{h} e^{\mathbf{A}_c s} ds \mathbf{B}_c$, $\widehat{\mathbf{E}}_0 = \mathbf{B}_c$, $\widehat{\mathbf{D}} = \beta e^{\mathbf{A}_c (h/2)}$, $\mathbf{F}(\tau_k) = \beta^{-1} \int_0^{-\widehat{\tau}_k} e^{\mathbf{A}_c s} ds$, and $\beta = \max_{\widehat{\tau}_k} \| \int_0^{-\widehat{\tau}_k} e^{\mathbf{A}_c s} ds \|_2 = \| \int_0^{h/2} e^{\mathbf{A}_c s} ds \|_2$. It is obvious that $\mathbf{F}^T(\tau_k)\mathbf{F}(\tau_k) \le \mathbf{I}$, then $\mathbf{\Gamma}_0(h,\tau_k)$ and $\mathbf{\Gamma}_1(h,\tau_k)$ can be rewritten as

$$\mathbf{\Gamma}_0(h,\tau_k) = \widehat{\mathbf{\Gamma}}_0 + \widehat{\mathbf{D}}\mathbf{F}(\tau_k)\widehat{\mathbf{E}}_0 \tag{7}$$

$$\mathbf{\Gamma}_1(h,\tau_k) = \widehat{\mathbf{\Gamma}}_1 - \widehat{\mathbf{D}}\mathbf{F}(\tau_k)\widehat{\mathbf{E}}_0 \tag{8}$$

Put (7) and (8) into (5), and $\mathbf{A}_{d1}$ and $\mathbf{B}_{d1}$ can be rewritten as

$$\begin{aligned}\mathbf{A}_{d1} &= \widehat{\mathbf{A}}_{d1} + \mathbf{D}\mathbf{F}(\tau_k)\mathbf{E}_a \\ &= \begin{bmatrix}\mathbf{\Phi}(h) & \widehat{\mathbf{\Gamma}}_1 \\ \mathbf{0} & \mathbf{0}\end{bmatrix} + \begin{bmatrix}\widehat{\mathbf{D}} \\ \mathbf{0}\end{bmatrix}\mathbf{F}(\tau_k)\begin{bmatrix}\mathbf{0} & \widehat{\mathbf{E}}_0\end{bmatrix} \\ \mathbf{B}_{d1} &= \widehat{\mathbf{B}}_{d1} + \mathbf{D}\mathbf{F}(\tau_k)\mathbf{E}_b = \begin{bmatrix}\widehat{\mathbf{\Gamma}}_0 \\ \mathbf{I}\end{bmatrix} + \begin{bmatrix}\widehat{\mathbf{D}} \\ \mathbf{0}\end{bmatrix}\mathbf{F}(\tau_k)\left(-\widehat{\mathbf{E}}_0\right)\end{aligned} \tag{9}$$

The uncertain item $\mathbf{F}(\tau_k)$ in (7) and (8) can be tackled by the theorem proposed in the next section.

3. Codesign of the Robust Event-Triggered Controller and Dynamic Scheduler

We employ a quadratic triggering condition introduced in [21] as follows:

$$\mathbf{z}^T(k)\mathbf{M}_1\mathbf{z}(k) - \mathbf{z}^T(k-1)\mathbf{M}_2\mathbf{z}(k-1) > 0 \tag{10}$$

where M_1 and M_2 are symmetric and positive matrices.

Equation (10) makes the data transmission of the control loop been triggered only when the weighted Euclidean norm

of the current states of the plant is larger than the previous ones which always means that the control performances are getting worse.

Therefore, the event generator considered implements a discrete-time event-triggered law as follows:

$$\sigma(k) := \hat{\mathbf{z}}^T(k)\,\mathbf{M}\hat{\mathbf{z}}(k) > 0 \tag{11}$$

where

$$\hat{\mathbf{z}}(k) = \left(\mathbf{z}^T(k) \;\; \mathbf{z}^T(k-1)\right)^T, \qquad \mathbf{M} = \operatorname{diag}\left(\mathbf{M}_1, -\mathbf{M}_2\right). \tag{12}$$

Letting $\sigma_i(k)$ denote the event generator implemented in control loop i and considering that there are more than one control loop satisfying the data transmission triggering condition, we need a scheduling strategy to arbitrate the priority of accessing the network. We present the dynamic scheduling strategy based on the event-trigger law in (11) as

$$\delta(k) = \begin{cases} \arg\max\limits_{i\in\{1,\ldots,N\}} \sigma_i(k) & \text{otherwise} \\ 0 & \text{if } \sigma_i(k) \le 0 \;\forall i \end{cases} \tag{13}$$

where $\sigma_i(k)$ denotes the corresponding event generator and N represents the control loop number in the NCS.

$\delta(k)$ guarantees the control loop with the largest weighted Euclidean norm of the states, namely, the control loop with worst control performances having the authority to access the network. In addition, $\delta(k) = 0$ means that there is no control loop need to access the network at the current instant.

Considering the event generator in (11), (5) and (6) can be written as

$$\mathbf{z}(k+1) = \begin{cases} \mathbf{A}_{d1}\mathbf{z}(k) + \mathbf{B}_{d1}\mathbf{u}(k) & \text{if } \hat{\mathbf{z}}^T(k)\,\mathbf{M}\hat{\mathbf{z}}(k) > 0 \\ \mathbf{A}_{d2}\mathbf{z}(k) + \mathbf{B}_{d2}\mathbf{u}(k) & \text{otherwise} \end{cases} \tag{14}$$

where

$$\mathbf{A}_{d1} = \widehat{\mathbf{A}}_{d1} + \mathbf{DF}(\tau_k)\,\mathbf{E}_a, \qquad \mathbf{B}_{d1} = \widehat{\mathbf{B}}_{d1} + \mathbf{DF}(\tau_k)\,\mathbf{E}_b. \tag{15}$$

Considering the closed loop, the quadratic performance cost function is as follows:

$$J = \sum_{k=0}^{\infty} \mathbf{x}^T(k)\,\mathbf{Q}\mathbf{x}(k) + \mathbf{u}^T(k)\,\mathbf{R}\mathbf{u}(k) \tag{16}$$

where $\mathbf{Q}$ and $\mathbf{R}$ are the positive definite symmetric weight matrices. The event-based codesign problem with guaranteed control performances in our work is thus described as follows.

Design a state feedback control law and an event-triggering law, namely, the matrix $\mathbf{M}$ in (11) to guarantee the switched system formulated in (14) globally uniformly asymptotically stable and to make the closed-loop quadratic performance cost meet

$$J \le \mathbf{z}^T(0)\,\mathbf{P}\mathbf{z}(0) \tag{17}$$

where P is a symmetric positive definite matrix.

The following theorem could be used to tackle the codesign problem above.

Theorem. Given a scalar $\varepsilon > 0$, the solution to the problem mentioned above could be achieved if there exist symmetric positive definite matrices $\mathbf{X}$, $\mathbf{Y}$, $\mathbf{N_1}$, $\mathbf{M_2}$ and matrix $\mathbf{W}$ with compatible dimension such that

$$\begin{bmatrix} -\mathbf{N}_1 & * & * & * & * & * & * \\ \mathbf{0} & -\mathbf{R}^{-1} & * & * & * & * & * \\ \mathbf{0} & \mathbf{0} & -\mathbf{Q}^{-1} & * & * & * & * \\ \mathbf{0} & \mathbf{0} & \mathbf{0} & -\mathbf{Y} & * & * & * \\ \mathbf{0} & \mathbf{0} & \mathbf{0} & \mathbf{0} & -\varepsilon\mathbf{I} & * & * \\ \mathbf{0} & \mathbf{0} & \mathbf{0} & \mathbf{0} & \mathbf{0} & -\mathbf{X} + \varepsilon\widetilde{\mathbf{D}}\widetilde{\mathbf{D}}^T & * \\ \mathbf{X} & \mathbf{W}^T & \mathbf{X} & \mathbf{X} & \left(\mathbf{E}_a\mathbf{X} + \mathbf{E}_b\mathbf{W}\right)^T & \left(\widehat{\mathbf{A}}_{d1}\mathbf{X} + \widehat{\mathbf{B}}_{d1}\mathbf{W}\right)^T & -\mathbf{X} \end{bmatrix} < 0 \tag{18}$$

$$-2\mathbf{I} + \mathbf{Y} - \mathbf{M}_2 < 0 \tag{19}$$

$$\begin{bmatrix} -\mathbf{R}^{-1} & * & * & * & * \\ \mathbf{0} & -\mathbf{Q}^{-1} & * & * & * \\ \mathbf{0} & \mathbf{0} & -\mathbf{Y} & * & * \\ \mathbf{0} & \mathbf{0} & \mathbf{0} & -\mathbf{X} & * \\ \mathbf{W}^T & \mathbf{X} & \mathbf{X} & \left(\mathbf{A}_{d2}\mathbf{X} + \mathbf{B}_{d2}\mathbf{W}\right)^T & -3\mathbf{X} + \mathbf{N}_1 \end{bmatrix} < 0 \tag{20}$$

$$-2\mathbf{I} + \mathbf{Y} + \mathbf{M}_2 < 0 \tag{21}$$

hold, where $*$ denotes the symmetrical element.

We implement the full state feedback control law for system equation (14) as $\mathbf{u}(k) = \mathbf{K}\mathbf{z}(k)$; thus, the state feedback gain $\mathbf{K}$ and the event-triggering law $\mathbf{M}$ can be solved as finding the solutions of $\mathbf{X}$, $\mathbf{Y}$, $\mathbf{N_1}$, $\mathbf{M_2}$, $\mathbf{W}$ in LMIs equations (18), (19), (20), and (21), and then $\mathbf{K} = \mathbf{W}\mathbf{X}^{-1}$, $\mathbf{M} = \mathrm{diag}(\mathbf{N_1}^{-1}, -\mathbf{M_2})$, and the corresponding close-loop cost function satisfies

$$J \le \mathbf{z}^T(0)\left(\mathbf{X}^{-1}\right)\mathbf{z}(0) \tag{22}$$

Proof. The detailed proof can be found in Appendix. □

4. Experiment Results

In this section, the effectiveness of the proposed codesign strategies is evaluated via a networked control system. The system consists of three inverted pendulums shared a controller via network whose topology is shown in Figure 1. A Matlab-based toolbox Truetime [25] is employed to implement the simulation experiments. The linearized state equation of the inverted pendulum $\mathbf{P}_i$ $(i \in \{1, 2, 3\})$ is given by

$$\begin{aligned}\dot{\mathbf{x}}_i &= \begin{bmatrix} 0 & 1 \\ \dfrac{(m_i + M_i)\, g}{M_i l_i} & 0 \end{bmatrix} \mathbf{x}_i \\ &\quad + \begin{bmatrix} 0 \\ \dfrac{1}{M_i l_i} \end{bmatrix} \left(u_i(t - \tau_i(t)) + f_i(t)\right)\end{aligned} \tag{23}$$

where $\mathbf{x}_i = \left[\phi_i \;\; \dot{\phi}_i\right]^T$, ϕ_i denotes the pendulum angle, $u_i(t)$ is the force acting on the cart, and $f_i(t)$ is a force disturbance. $\tau_i(t)$ is the uncertain time-varying delay induced by the bandwidth competition. The m_i and M_i represent the pendulum mass and the cart mass of plant i, respectively, and l_i means the pendulum length. Here, we set that $m_i = 0.3kg$ and $M_i = 0.1kg$ for $i \in \{1, 2, 3\}$, $l_{1/2/3} = 0.8/1.2/1.5m$.

The sampling period h_i of each sensor should be chosen according to the constraints caused by control performances and the bandwidth scheduling. The upper bound of h_i can be obtained from stability conditions of control systems, e.g., the method presented by reference [26]. Although a shorter sampling period is preferable in most control systems, too short sampling period may lead to overloading of network which always causes the degradation of control performances. Therefore, the lower bound of h_i should be restricted by the schedulability of given scheduling strategies such as RM (Rate Monotonic) or EDF (Earliest Deadline First) which can guarantee $\tau_i(t) \le h_i$ when all the control loops require the network accession simultaneously. Assuming that the length of the packet carrying sample or control update message is 320 *bits*. When the transmission rate of the network is 100 *kbits/s*, it will takes 3.2 *ms* to the transmit the packet. We choose sample periods $h_1 = 20ms, h_2 = 30ms, h_3 = 40ms$ to satisfy the schedulability constraint for RM [27]as

$$\sum_{i=1}^{N} \frac{(tc_i + ts_i)}{h_i} < N\left(2^{1/N} - 1\right) \tag{24}$$

where $ts_i = 3.2ms$,$tc_i = 3.2ms$ represent the transmission time for sample and control packet respectively and $N = 3$ denotes the number of the control loop.

It is should be noticed that, under the periodic event-triggered strategies [16], the new states of plant are measured at each sampling period by sensors, whether performing transmissions of the measurements and control updates are triggered only when it is necessary because of the control performance formulated by (11).

Forwarding the model parameters into (14) and letting $\mathbf{Q}$ and $\mathbf{R}$ from (16) be unit matrices, solving LMIs equations (18)−Eq.(21) yields both the feasible control gain matrices

$$\begin{aligned}\mathbf{K}_1 &= (-5.4851, -0.7796, -0.0149) \\ \mathbf{K}_2 &= (-5.4140, -0.9449, -0.0287) \\ \mathbf{K}_3 &= (-5.2172, -1.0195, -0.0943)\end{aligned} \tag{25}$$

and the event generator weight matrix in (11) (taking control loop P_1, for example):

$$\mathbf{M} = \begin{bmatrix} 7.5755 & * & * & * & * & * \\ 1.0471 & 0.3502 & * & * & * & * \\ 0.3296 & 0.1540 & 0.1687 & * & * & * \\ 0 & 0 & 0 & 6.0604 & * & * \\ 0 & 0 & 0 & 0.8377 & 0.2802 & * \\ 0 & 0 & 0 & 0.2637 & 0.1232 & 0.1349 \end{bmatrix} \tag{26}$$

For the purpose of estimating the performance of the proposed strategy, we set the initial states and the force disturbances of the plants as follows:

$$\begin{aligned}&\begin{bmatrix} \phi_1(0) \\ \dot{\phi}_1(0) \end{bmatrix} = \begin{bmatrix} \dfrac{\pi}{4} \\ 0.0 \end{bmatrix}, \\ &f_1(t) = 0.0 \\ &\begin{bmatrix} \phi_2(0) \\ \dot{\phi}_2(0) \end{bmatrix} = \begin{bmatrix} \dfrac{\pi}{12} \\ 0.0 \end{bmatrix}, \\ &f_2(t) = \begin{cases} 1.0 & t = 3^{th}s \\ 0.0 & otherwise \end{cases} \\ &\begin{bmatrix} \phi_3(0) \\ \dot{\phi}_3(0) \end{bmatrix} = \begin{bmatrix} \dfrac{\pi}{36} \\ 0.0 \end{bmatrix}, \\ &f_3(t) = \begin{cases} -0.8 & t = 8^{th}s \\ 0.8 & t = 10^{th}s \\ 0.0 & otherwise \end{cases}\end{aligned} \tag{27}$$

Figure 2 shows the responses of the control loops with the initial states and impulsive force disturbances in (27). Figure 3

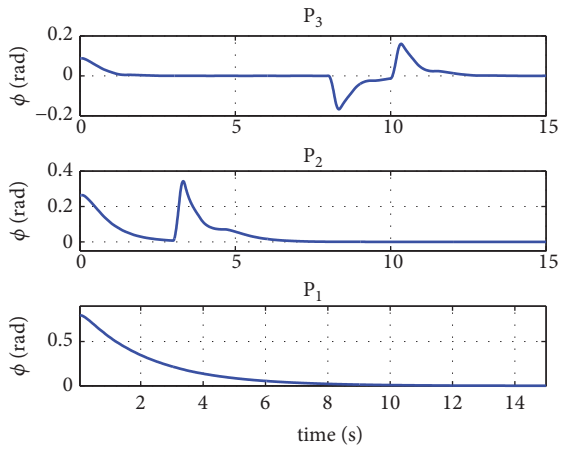

Figure 2: The response of the pendulum angle.

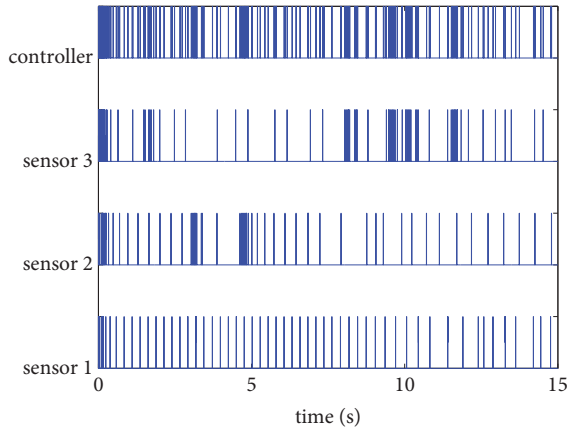

Figure 3: Message transmission under event driven with average resource utilization 14.5%.

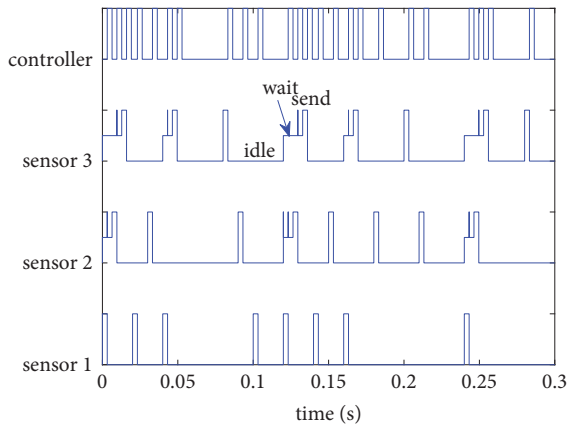

Figure 4: Message transmission $t \in [0.0, 0.5]$.

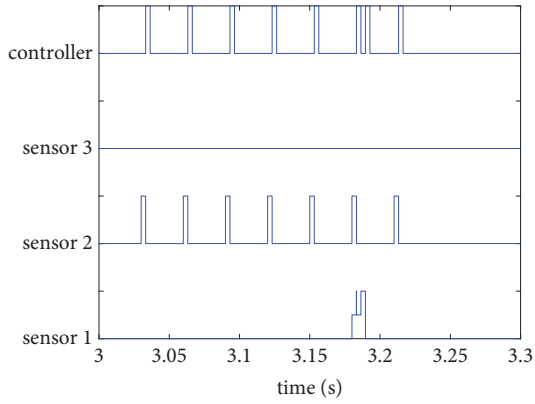

Figure 5: Message transmission $t \in [3.0, 3.3]$.

shows the corresponding message transmission through the network. All the control loops send the measurement packets through the network with short intervals at the beginning of simulation since all the inverted pendulums are subject to the disturbance caused by the initial states. When $t \in [3.0s, 3.3s]$, control loop P_2 has more chance to access the network because P_2 is subject to an impulsive force disturbance emerging at $3^{th}s$, and the pendulum angle deviates the equilibrium. The corresponding control task is triggered frequently to adjust the system back to its equilibrium. Similarly, when $t \in [8.0s, 12.0s]$, control loop P_3 accesses the network more frequently because P_3 is subject to an impulsive force disturbance emerged at $8^{th}s$ and $10^{th}s$. Meanwhile, one can also notice that when P_i converges to its equilibrium, the packets transmission interval is expended to save the bandwidth resource. It is clear that the proposed event-triggered control and scheduling strategies allocate the network resource according to the needs of the plant and keep the whole system stable with only 17.9% of average resource utilization and 66.7% of peak resource utilization.

Figures 4 and 5 demonstrate the scheduling details when there are multiple transmission requests occurring simultaneously. In Figure 4, when $t \in [0.0s, 0.3s]$, P_1 has the maximum pendulum angle error form equilibrium; therefore, the control loop 1 has the highest network accession authority (no waiting when the transmission is triggered) according to the scheduling strategy in (13), whereas, in Figure 5, when $t \in [3.0s, 3.3s]$, P_2 is subject to the impulse force disturbance, and the control loop 2 gets the highest authority to access the network.

To compare the performance of time-driven based and event-driven based control strategies, we run another simulated experiment. Considering the inverted pendulum P_3 under the impulsive force disturbance shown in (27), for example, we choose the sample pocket transmission periods with resource utilization 30% and 69.3% and implement time-driven data transmission shown in Figure 6; by designing a cost guaranteed control law with uncertain delay [28], the quadratic performance formulated in (16) under the time-driven versus the proposed event-driven codesign framework is recorded and shown in Figure 7.

It is obvious that the proposed event-driven approach with the average resource utilization 14.5% obtains almost the same quadratic performance as the time-driven approach with resource utilization 69.3%. And it obtains better control performances than the time-driven approach with resource utilization 30%. That is, the proposed event-driven approach

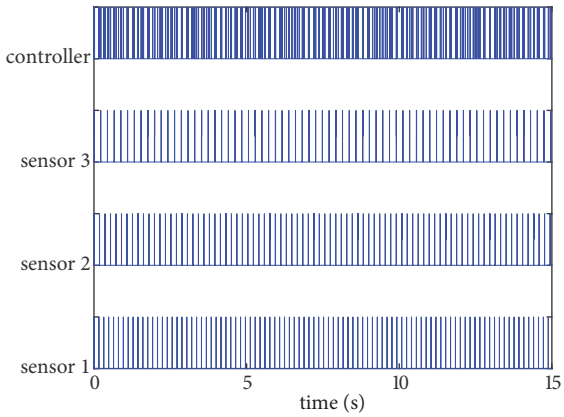

Figure 6: Message transmission under time driven with average resource utilization 30.0%.

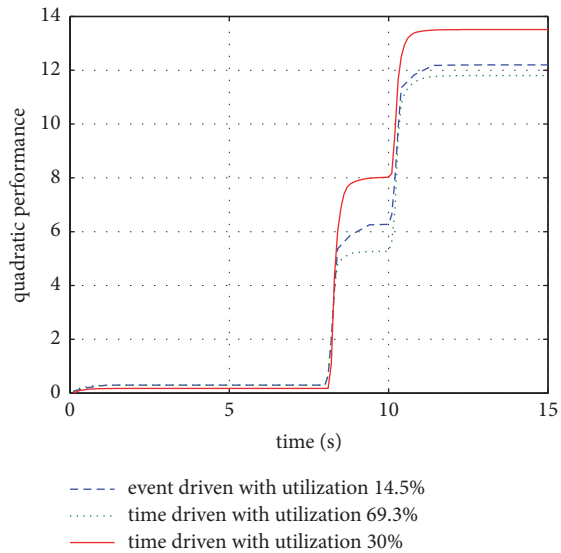

Figure 7: The comparison of quadratic performance between time-driven strategy and event-driven strategy.

can obtain better control performances with a low resource utilization.

5. Conclusions

For an efficient usage of the limited bandwidth resources in NCSs, an event-triggered scheduling and control codesign approach has been proposed. The approach employs a scheduler to handle the resources distribution problem and employs an event generator to tackle the resources utilization problem. By modeling the event-based networked control system as a switched discrete system with uncertain parameters, the controller, scheduler, and event generator are jointly designed by solving a set of LMIs. The results of experiments clearly demonstrated that the proposed event-based codesign approach makes all the control loops in NCS stable and achieves better control performances with low resource consumption.

We also notice that, in view of existing results, the potential methods for robust control of uncertain parameter systems are the common quadratic Lyapunov function based (CQLF) approaches and the parameter dependent Lyapunov function based (PDLF) approaches [29]. Comparing with PQLF approaches, the CDLF approaches may lead to different degrees of conservativeness due to the use of a single Lyapunov function for the entire set of uncertainties. Since the transmission delay τ_k can be bounded and estimated by the General Time-Demand Analysis Method [27] and (13) can also be equivalently represented by a linear polytopic form, we will focus on doing further researches about the event-triggered gain-scheduled control and bandwidth scheduling codesign based on PQLF approaches to obtain some less conservative results in our future work.

Appendix

Proof of the Theorem

To prove the proposed theorem, the following lemmas [28] is required.

Lemma A.1. *The following LMIs are equivalent:*

$$\begin{aligned} \begin{bmatrix} \mathbf{Q} & \mathbf{S} \\ \mathbf{S}^{\mathbf{T}} & \mathbf{R} \end{bmatrix} &< 0 \\ \mathbf{Q} &< 0, \\ \mathbf{R} - \mathbf{S}^T\mathbf{Q}^{-1}\mathbf{S} &< 0 \\ \mathbf{R} &< 0, \\ \mathbf{Q} - \mathbf{S}\mathbf{R}^{-1}\mathbf{S}^T &< 0 \end{aligned} \tag{A.1}$$

Lemma A.2. *Let* $\mathbf{Y}$, $\mathbf{M}$, $\mathbf{N}$ *be given constant matrices of compatible dimension, then for any uncertain matrix* $\mathbf{F}$ *satisfying* $\mathbf{F}^T\mathbf{F} \le \mathbf{I}$,

$$\mathbf{Y} + \mathbf{MFN} + \mathbf{N}^T\mathbf{F}^T\mathbf{M}^T < 0 \tag{A.2}$$

holds if and only if there exists a scalar $\varepsilon > 0$ *such that*

$$\mathbf{Y} + \varepsilon\mathbf{M}\mathbf{M}^T + \varepsilon^{-1}\mathbf{N}^T\mathbf{N} < 0 \tag{A.3}$$

Proof of the Theorem. Considering (14) and employing the state feedback control law $\mathbf{u}(k) = \mathbf{Kz}(k)$, the closed-loop system equation can be written as

$$\mathbf{z}(k+1) = \begin{cases} \widetilde{\mathbf{A}}_{d1}\mathbf{z}(k) & \text{if } \hat{\mathbf{z}}^T(k)\,\mathbf{M}\hat{\mathbf{z}}(k) > 0 \\ \widetilde{\mathbf{A}}_{d2}\mathbf{z}(k) & \text{otherwise} \end{cases} \tag{A.4}$$

where $\widetilde{\mathbf{A}}_{d1} = \mathbf{A}_{d1} + \mathbf{B}_{d1}\mathbf{K}$, $\widetilde{\mathbf{A}}_{d2} = \mathbf{A}_{d2} + \mathbf{B}_{d2}\mathbf{K}$.

We choose a Lyapunov function as follows:

$$V(k) = \mathbf{z}^T(k)\,\mathbf{P}_1\mathbf{z}(k) + \mathbf{z}^T(k-1)\,\mathbf{P}_2\mathbf{z}(k-1) \tag{A.5}$$

where $\mathbf{P}_1$ and $\mathbf{P}_2$ are symmetric and positive definite matrices.

$\Delta V(k) = V(k+1) - V(k)$ meets

$$\Delta V(k) < -\mathbf{z}^T(k)\left(\mathbf{Q} + \mathbf{K}^T\mathbf{R}\mathbf{K}\right)\mathbf{z}(k) < 0 \tag{A.6}$$

where $\mathbf{Q}$ and $\mathbf{R}$ are the weight matrices in (16).

The system equation (A.4) is asymptotically stable; meanwhile, the quadratic performance defined in (16) meets

$$J \le V(0) = \mathbf{z}^T(0)\,\mathbf{P}_1\mathbf{z}(0) \tag{A.7}$$

In case of $\hat{\mathbf{z}}^T(k)\mathbf{M}\hat{\mathbf{z}}(k) > 0$, by putting (A.4) into (A.6), we have

$$\Delta V(k) = \hat{\mathbf{z}}^T(k)\begin{bmatrix}\prod & \mathbf{0}\\ \mathbf{0} & -\mathbf{P}_2\end{bmatrix}\hat{\mathbf{z}}(k) < 0 \tag{A.8}$$

where $\prod = \widetilde{\mathbf{A}}_{d1}^T\mathbf{P}_1\widetilde{\mathbf{A}}_{d1} - \mathbf{P}_1 + \mathbf{P}_2 + \mathbf{Q} + \mathbf{K}^T\mathbf{R}\mathbf{K}$.

Considering $\mathbf{M} = \operatorname{diag}(\mathbf{M}_1, -\mathbf{M}_2)$, according to the S-procedure [30], (A.8) with constraint $\hat{\mathbf{z}}^T(k)\mathbf{M}\hat{\mathbf{z}}(k) > 0$ holds if

$$\hat{\mathbf{z}}^T(k)\left(\begin{bmatrix}\prod & \mathbf{0}\\ \mathbf{0} & -\mathbf{P}_2\end{bmatrix} + \lambda\begin{bmatrix}\mathbf{M}_1 & \mathbf{0}\\ \mathbf{0} & -\mathbf{M}_2\end{bmatrix}\right)\hat{\mathbf{z}}(k) < 0 \tag{A.9}$$

where λ is a nonnegative real scalar parameter which could be used to obtain the less conservative results by finding the smallest volume ellipsoid containing the union of ellipsoids which hold the LMI above [30]. When $\lambda = 1$, the smallest volume ellipsoid can be found. Thus we have

$$\begin{bmatrix}\Pi + \mathbf{M}_1 & \mathbf{0}\\ \mathbf{0} & -\mathbf{P}_2 - \mathbf{M}_2\end{bmatrix} < 0 \tag{A.10}$$

Equation (A.10) is equivalent to

$$\widetilde{\mathbf{A}}_{d1}^T\mathbf{P}_1\widetilde{\mathbf{A}}_{d1} - \mathbf{P}_1 + \mathbf{P}_2 + \mathbf{Q} + \mathbf{K}^T\mathbf{R}\mathbf{K} + \mathbf{M}_1 < 0 \tag{A.11}$$

$$-\mathbf{P}_2 - \mathbf{M}_2 < 0 \tag{A.12}$$

By applying Lemma A.1 to (A.11) and put (5) into (A.4), we have

$$\begin{bmatrix}-\mathbf{P}_1^{-1} & *\\ \left(\widehat{\mathbf{A}}_{d1} + \widehat{\mathbf{B}}_{d1}\mathbf{K}\right)^T & \Pi_1\end{bmatrix} + \Pi_2 < 0 \tag{A.13}$$

where

$$\Pi_1 = -\mathbf{P}_1 + \mathbf{P}_2 + \mathbf{Q} + \mathbf{K}^T\mathbf{R}\mathbf{K} + \mathbf{M}_1$$

$$\Pi_2 = \begin{bmatrix}\mathbf{D}\\ \mathbf{0}\end{bmatrix}\mathbf{F}(\tau)\begin{bmatrix}\mathbf{0} & \mathbf{E}_k\end{bmatrix} + \begin{bmatrix}\mathbf{0} & \mathbf{E}_k\end{bmatrix}^T\mathbf{F}^T(\tau)\begin{bmatrix}\mathbf{D}\\ \mathbf{0}\end{bmatrix}^T \tag{A.14}$$

$$\mathbf{E}_k = \mathbf{E}_a + \mathbf{E}_b\mathbf{K}$$

According to Lemma A.2, (A.13) holds if and only if there exists a scalar ε such that

$$\begin{bmatrix}-\mathbf{P}_1^{-1} + \varepsilon\mathbf{D}\mathbf{D}^T & *\\ \left(\widehat{\mathbf{A}}_{d1} + \widehat{\mathbf{B}}_{d1}\mathbf{K}\right)^T & \Pi_1\end{bmatrix} + \varepsilon^{-1}\begin{bmatrix}\mathbf{0}\\ \mathbf{E}_k^T\end{bmatrix}\begin{bmatrix}\mathbf{0} & \mathbf{E}_k\end{bmatrix} < 0 \tag{A.15}$$

By applying Lemma A.1 to eliminate the element ε^{-1} in (A.15), we have

$$\begin{bmatrix}-\varepsilon\mathbf{I} & * & *\\ \mathbf{0} & -\mathbf{P}_1^{-1} + \varepsilon\mathbf{D}\mathbf{D}^T & *\\ \mathbf{E}_k^T & \left(\widehat{\mathbf{A}}_{d1} + \widehat{\mathbf{B}}_{d1}\mathbf{K}\right)^T & \Pi_1\end{bmatrix} < 0 \tag{A.16}$$

Let $\mathbf{X} = \mathbf{P}_1^{-1}$ and multiply $\operatorname{diag}(\mathbf{I}, \mathbf{I}, \mathbf{X})$ to both sides of (A.16), we have

$$\begin{bmatrix}-\varepsilon\mathbf{I} & * & *\\ \mathbf{0} & -\mathbf{X} + \varepsilon\mathbf{D}\mathbf{D}^T & *\\ (\mathbf{E}_k\mathbf{X})^T & \left(\widehat{\mathbf{A}}_{d1}\mathbf{X} + \widehat{\mathbf{B}}_{d1}\mathbf{K}\mathbf{X}\right)^T & \Pi_3\end{bmatrix} < 0 \tag{A.17}$$

where

$$\Pi_3 = -\mathbf{X} + \mathbf{X}\mathbf{P}_2\mathbf{X} + \mathbf{X}\mathbf{Q}\mathbf{X} + (\mathbf{K}\mathbf{X})^T\mathbf{R}(\mathbf{K}\mathbf{X}) + \mathbf{X}\mathbf{M}_1\mathbf{X} \tag{A.18}$$

By applying Lemma A.1 to $\mathbf{P}_2$, $\mathbf{Q}$, $\mathbf{R}$, and $\mathbf{M}_1$ in (A.17), we have that (A.17) holds if and only if

$$\begin{bmatrix}-\mathbf{M}_1^{-1} & * & * & * & * & * & *\\ \mathbf{0} & -\mathbf{R}^{-1} & * & * & * & * & *\\ \mathbf{0} & \mathbf{0} & -\mathbf{Q}^{-1} & * & * & * & *\\ \mathbf{0} & \mathbf{0} & \mathbf{0} & -\mathbf{P}_2^{-1} & * & * & *\\ \mathbf{0} & \mathbf{0} & \mathbf{0} & \mathbf{0} & -\varepsilon\mathbf{I} & * & *\\ \mathbf{0} & \mathbf{0} & \mathbf{0} & \mathbf{0} & \mathbf{0} & -\mathbf{X} + \varepsilon\widetilde{\mathbf{D}}\widetilde{\mathbf{D}}^T & *\\ \mathbf{X} & (\mathbf{K}\mathbf{X})^T & \mathbf{X} & \mathbf{X} & (\mathbf{E}_k\mathbf{X})^T & \left(\widehat{\mathbf{A}}_{d1}\mathbf{X} + \widehat{\mathbf{B}}_{d1}\mathbf{K}\mathbf{X}\right)^T & -\mathbf{X}\end{bmatrix} < 0 \tag{A.19}$$

Letting $\mathbf{N}_1 = \mathbf{M}_1{}^{-1}$, $\mathbf{Y} = \mathbf{P}_2{}^{-1}$, $\mathbf{W} = \mathbf{KX}$ and considering $\mathbf{E}_k = \mathbf{E}_a + \mathbf{E}_b\mathbf{K}$, (A.17) is equivalent to (18).

Considering $\mathbf{Y} = \mathbf{P}_2{}^{-1}$, (A.12) is written as

$$-\mathbf{Y}^{-1} - \mathbf{M}_2 < 0 \tag{A.20}$$

Because $\mathbf{Y}$ is not negatively definite, Lemma A.1 is not applicable to eliminate $\mathbf{Y}^{-1}$ in (A.20). However, since $\mathbf{Y}^{-1} > 0$, then

$$(\mathbf{Y} - \mathbf{S})^T \mathbf{Y}^{-1} (\mathbf{Y} - \mathbf{S}) > 0 \tag{A.21}$$

holds, where $\mathbf{S}$ is a matrix with compatible dimension. And since $\mathbf{Y}$ is symmetric, (A.21) is equivalent to

$$\mathbf{S}^T\mathbf{Y}^{-1}\mathbf{S} \geq \mathbf{S}^T + \mathbf{S} - \mathbf{Y} \tag{A.22}$$

Here, let $\mathbf{S} = \mathbf{I}$, and then we have

$$\mathbf{Y}^{-1} \geq 2\mathbf{I} - \mathbf{Y} \tag{A.23}$$

According to (A.23), it is obvious that (A.20) holds if

$$-2\mathbf{I} + \mathbf{Y} - \mathbf{M}_2 < 0 \tag{A.24}$$

Comparing (A.19) and (A.24) with (18) and (19), respectively, the theorem is partly proved.

Similarly, applying the S-procedure to $\Delta V(k)$ with constraint $\hat{\mathbf{z}}^T(k)\mathbf{M}\hat{\mathbf{z}}(k) \leq 0$, we have

$$\hat{\mathbf{z}}^T(k)\left(\begin{bmatrix}\mathbf{\Lambda} & \mathbf{0}\\ \mathbf{0} & -\mathbf{P}_2\end{bmatrix} - \lambda\begin{bmatrix}\mathbf{M}_1 & \mathbf{0}\\ \mathbf{0} & -\mathbf{M}_2\end{bmatrix}\right)\hat{\mathbf{z}}(k) < 0 \tag{A.25}$$

where $\mathbf{\Lambda} = \widetilde{\mathbf{A}}_{d2}^T\mathbf{P}_1\widetilde{\mathbf{A}}_{d2} - \mathbf{P}_1 + \mathbf{P}_2 + \mathbf{Q} + \mathbf{K}^T\mathbf{RK}$; λ can be a nonnegative real scalar. By setting $\lambda = 1$, the inequality holds if

$$\widetilde{\mathbf{A}}_{d2}^T\mathbf{P}_1\widetilde{\mathbf{A}}_{d2} - \mathbf{P}_1 + \mathbf{P}_2 + \mathbf{Q} + \mathbf{K}^T\mathbf{RK} - \mathbf{M}_1 < 0 \tag{A.26}$$

$$-\mathbf{P}_2 + \mathbf{M}_2 < 0 \tag{A.27}$$

By applying Lemma A.1 repeatedly to (A.26) and employing the substitution $\mathbf{N}_1 = \mathbf{M}_1{}^{-1}$, $\mathbf{Y} = \mathbf{P}_2{}^{-1}$, $\mathbf{W} = \mathbf{KX}$, we have

$$\begin{bmatrix}-\mathbf{R}^{-1} & * & * & * & *\\ \mathbf{0} & -\mathbf{Q}^{-1} & * & * & *\\ \mathbf{0} & \mathbf{0} & -\mathbf{Y} & * & *\\ \mathbf{0} & \mathbf{0} & \mathbf{0} & -\mathbf{X} & *\\ \mathbf{W}^T & \mathbf{X} & \mathbf{X} & (\mathbf{A}_{d2}\mathbf{X} + \mathbf{B}_{d2}\mathbf{W})^T & -\mathbf{X} - \mathbf{X}\mathbf{N}_1{}^{-1}\mathbf{X}\end{bmatrix} < 0 \tag{A.28}$$

Note that Lemma A.1 is not suitable to handle the item $-\mathbf{X} - \mathbf{X}\mathbf{N}_1{}^{-1}\mathbf{X}$ because of the positive definiteness of $\mathbf{N}_1{}^{-1}$. However, applying the similar procedure shown in (A.21) and (A.22), we have

$$\mathbf{X}\mathbf{N}_1{}^{-1}\mathbf{X} \geq \mathbf{X} + \mathbf{X} - \mathbf{N}_1 \tag{A.29}$$

It means that (A.28) holds if

$$\begin{bmatrix}-\mathbf{R}^{-1} & * & * & * & *\\ \mathbf{0} & -\mathbf{Q}^{-1} & * & * & *\\ \mathbf{0} & \mathbf{0} & -\mathbf{Y} & * & *\\ \mathbf{0} & \mathbf{0} & \mathbf{0} & -\mathbf{X} & *\\ \mathbf{W}^T & \mathbf{X} & \mathbf{X} & (\mathbf{A}_{d2}\mathbf{X} + \mathbf{B}_{d2}\mathbf{W})^T & -3\mathbf{X} + \mathbf{N}_1\end{bmatrix} < 0 \tag{A.30}$$

Similar to the procedure to handle (A.20), (A.27) holds if

$$-2\mathbf{I} + \mathbf{Y} + \mathbf{M}_2 < 0 \tag{A.31}$$

Comparing LMIs (A.19), (A.24), (A.30), and (A.31) with (18), (19), (20), and (21), respectively, the proof of the theorem is completed. □

Data Availability

The data used to support the findings of this study are available from the corresponding author upon request.

Conflicts of Interest

The authors declare that they have no conflicts of interest.

Acknowledgments

This research was supported by Natural Science Basic Research Plan in Shaanxi Province of China (Program no. 2014JQ8346) and National Nature Science Foundation of China under Grant no. 61473224.

References

[1] R. A. Gupta and M. Y. Chow, "Networked control system: overview and research trends," *IEEE Transactions on Industrial Electronics*, vol. 57, no. 7, pp. 2527–2535, 2010.

[2] A. Cela, M. B. Gaid, X. G. Li, and S. I. Niculescu, "Optimal relation between quantization precision and sampling rates," *Communications and Control Engineering*, pp. 109–133, 2014.

[3] S. Al-Areqi, D. Gorges, and S. Liu, "Receding-horizon control and scheduling of systems with uncertain computation and communication delays," in *Proceedings of the 51st IEEE Conference on Decision and Control, CDC 2012*, pp. 2654–2659, USA, December 2012.

[4] R. Maestrelli, L. Almeida, D. Coutinho, and U. Moreno, "Dynamic bandwidth management in networked control systems using quantization," *ACM SIGBED Review*, vol. 11, no. 3, pp. 58–61, 2014.

[5] Z. Wang, H. Sun, and X. Zhang, "Multi-rate control and pole assignment for a single closed-loop in networked multi-rate control system," in *Proceedings of the 27th Chinese Control and Decision Conference, CCDC 2015*, pp. 6017–6021, China, May 2015.

[6] A. Cervin and P. Alriksson, "Optimal on-line scheduling of multiple control tasks: a case study," in *Proceedings of the 18th Euromicro Conference on Real-Time Systems, ECRTS 2006*, pp. 141–150, Germany, July 2006.

[7] S. Reimann, W. Wu, and S. Liu, "A novel control-schedule codesign method for embedded control systems," in *Proceedings of the 2012 American Control Conference, ACC 2012*, pp. 3766–3771, Canada, June 2012.

[8] C. Du, L. Tan, and Y. Dong, "Period selection for integrated controller tasks in cyber-physical systems," *Chinese Journal of Aeronautics*, vol. 28, no. 3, pp. 894–902, 2015.

[9] W. P. Heemels, J. H. Sandee, and P. P. J. van den Bosch, "Analysis of event-driven controllers for linear systems," *International Journal of Control*, vol. 81, no. 4, pp. 571–590, 2008.

[10] W. P. M. H. Heemels and M. C. F. Donkers, "Model-based periodic event-triggered control for linear systems," *Automatica*, vol. 49, no. 3, pp. 698–711, 2013.

[11] A. Girard, "Dynamic triggering mechanisms for event-triggered control," *IEEE Transactions on Automatic Control*, vol. 60, no. 7, pp. 1992–1997, 2015.

[12] R. Postoyan, P. Tabuada, D. Nesic, and A. Anta, "A framework for the event-triggered stabilization of nonlinear systems," *IEEE Transactions on Automatic Control*, vol. 60, no. 4, pp. 982–996, 2015.

[13] S. L. Hu, D. Yue, C. Peng, X. P. Xie, and X. X. Yin, "Event-triggered controller design of nonlinear discrete-time networked control systems in T-S fuzzy model," *Applied Soft Computing*, vol. 30, pp. 400–411, 2015.

[14] L. Zhang, X. Li, J. Yan, and X. Guan, "Event-triggered multi-target formation control for multiagent systems," *Mathematical Problems in Engineering*, vol. 2017, Article ID 1318376, 8 pages, 2017.

[15] V. S. Dolk, D. P. Borgers, and W. P. Heemels, "Output-based and decentralized dynamic event-triggered control with guaranteed lp-gain performance and zeno-freeness," *IEEE Transactions on Automatic Control*, vol. 62, no. 1, pp. 34–49, 2017.

[16] W. P. M. Heemels, M. C. F. Donkers, and A. R. Teel, "Periodic event-triggered control for linear systems," *IEEE Transactions on Automatic Control*, vol. 58, no. 4, pp. 847–861, 2013.

[17] A. Cervin and T. Henningsson, "Scheduling of event-triggered controllers on a shared network," in *Proceedings of the 47th IEEE Conference on Decision and Control, CDC 2008*, pp. 3601–3606, Mexico, December 2008.

[18] M. Rabi and K. H. Johansson, "Scheduling packets for event-triggered control," in *Proceedings of the 2009 10th European Control Conference, ECC 2009*, pp. 3779–3784, Hungary, August 2009.

[19] R. Blind, "Analysis of networked event-based control with a shared communication medium: part I – pure ALOHA," *IFAC Proceedings Volumes (IFAC-PapersOnline)*, vol. 18, no. 08, pp. 10092–10097, 2011.

[20] Q. L. Ma, C. Zhou, and L. L. Chen, "Co-design of event-trigger and quantized control for networked control systems," *Journal of The Franklin Institute*, vol. 218, no. 21, pp. 5844–5848, 2016.

[21] S. Al-Areqi, D. Görges, and S. Liu, "Event-based networked control and scheduling codesign with guaranteed performance," *Automatica*, vol. 57, pp. 128–134, 2015.

[22] T. Wang, C. Zhou, H. Lu, J. He, and J. Guo, "Hybrid scheduling and quantized output feedback control for networked control systems," *International Journal of Control Automation & Systems*, vol. 16, no. 1, pp. 197–206, 2018.

[23] W.-A. Zhang and L. Yu, "Modelling and control of networked control systems with both network-induced delay and packet-dropout," *Automatica*, vol. 44, no. 12, pp. 3206–3210, 2008.

[24] L. Hetel, J. Daafouz, and C. Iung, "Stabilization of arbitrary switched linear systems with unknown time-varying delays," *IEEE Transactions on Automatic Control*, vol. 51, no. 10, pp. 1668–1674, 2006.

[25] A. Cervin, H. Dan, and M. Ohlin, "Truetime 2.0 betaıreference manual," *Department of Automatic Control*, no. 1-2, pp. 67–81, 2012.

[26] D.-S. Kim, Y. S. Lee, W. H. Kwon, and H. S. Park, "Maximum allowable delay bounds of networked control systems," *Control Engineering Practice*, vol. 11, no. 11, pp. 1301–1313, 2003.

[27] C. M. Krishna, *Real-Time Systems*, Tsinghua University Pres, 2001.

[28] X. Li and C. E. de Souza, "Delay-dependent robust stability and stabilization of uncertain linear delay systems: a linear matrix inequality approach," *IEEE Transactions on Automatic Control*, vol. 42, no. 8, pp. 1144–1148, 1997.

[29] X. Zhao, L. Zhang, P. Shi, and H. Karimi, "Robust control of continuous-time systems with state-dependent uncertainties and its application to electronic circuits," *IEEE Transactions on Industrial Electronics*, vol. 61, no. 8, pp. 4161–4170, 2014.

[30] E. E. Yaz, "Linear matrix inequalities in system and control theory," *Proceedings of the IEEE*, vol. 86, no. 12, pp. 2473-2474, 1994.